AIAA-93-1487-CP

AN EXPERIMENTAL INVESTIGATION OF VIBRATION LOCALIZATION IN DISORDERED MULTI-§PAN BEAM§ *

Djamel Bouzit †
Christophe Pierre ‡

Department of Mechanical Engineering and Applied Mechanics
The University of Michigan
Ann Arbor, Michigan 48109-2125 U.S.A.

Abstract

The results of an experimental investigation of the effects of span length disorder on the dynamics of a mono-coupled, multi-span beam are reported. Two experimental specimen are considered: a nominally periodic twelve-span beam with equal spacing between simple supports, and the corresponding disordered beam which features slightly randomly spaced supports. Experimental results demonstrate that the transmission of vibration which takes place within the frequency passbands of the periodic beam is greatly hindered when span length randomness is introduced. The spatial localization of both the mode shapes and the steady-state harmonic response to an end excitation is observed in the disordered twelve-span beam, especially for frequencies which lie within the second passband. Very good quantitative agreement is obtained between experimental results and theoretical findings for both ordered and disordered configurations. Furthermore, an experimental estimation of the localization factor yields satisfactory agreement with the theoretical result for an infinite multi-span beam. This work reports one of the first systematic experiments carried out to demonstrate the Occurrence of vibration localization in nearly periodic structures.

1. Introduction

The phenomenon of vibration localization in nominally periodic structures has sparked much interest in the field of dynamics recently [1,2]. Spatially repetitive engineering structures are typically assumed to be made of identical substructures, or bays. While many useful results can be generated by a dynamics analysis which is based on the perfect periodicity assumption, it is now widely recognized that small, periodicity-breaking irregularities may cause the (sometimes severe) confinement of the vibration'al energy to small geometric regions of the structure.

A number of theoretical studies of the localization phenomenon were performed recently for various engineering structures (for example, see references [3,4,5]). Both deterministic analyses of the spatially localized free modes of disordered structures and statistical characterizations of the transmission of forced vibration from a local excitation source were conducted. These methodologies led to some general results regarding the effects of disorder. For example, localization was found to be most significant in nearly periodic structures with weak internal coupling, and the strength of localization was shown to increase with the disorder strength and generally with the frequency of excitation.

Strikingly few experiments were conducted in order to verify the analytical and numerical findings on localization in engineering structures. Hodges and Woodhouse [6] examined the dynamics of a taut string with attached masses. They studied the effect of unequal spacing of the beads by impacting the string near one end and comparing the portion of the incident energy reaching the other end for ordered and disordered configurations. Although their experiment evidenced vibration localization, the agreement between the spatial amplitude decay rates derived theoretically and experimentally was mostly qualitative.

Pierre *et* al. [7] demonstrated experimentally that localization occurs in beams on rigid supports, but only for a beam with two spans of unequal lengths. They achieved good quantitative agreement with the theoretically predicted modes.

Another interesting experiment was reported by Roy and Plunkett [8,9], one which concerned a supposedly periodic structure. Roy and Plunkett excited at one end a periodic beam with 15 cantilevers and, measuring its response, observed much more spatial attenuation experimentally than predicted by periodic theory. This leads us to believe that this discrepancy was caused by unaccounted localization effects which arose from an imperfect experimental specimen.

Finally, Levine-West and Salama [10] recently investigated experimentally the mode localization phenomenon in a full-scale 12-rib loosely-coupled antenna. They obtained a good agreement between numerical and experimental results, and thus provided strong evidence for the occurrence of localization in engineering systems.

Despite the availability of extensive theoretical results consolidated with numerical Monte Carlo simulations, we need experimental evidence of localization to (1) verify that localization occurs as predicted and (2) clarify our analytical

*This work was supported by NSF Grant No. MSS-8913196.
†Graduate Research Assistant, Member ASME.
‡Associate Professor, Member AIAA, ASME.

and numerical thinking of localization, particularly the effects of boundary conditions, damping, and individual realizations of disorder. As an attempt to meet this goal, the primary focus of this paper is a quantitative and systematic experimental verification of the occurrence of localization in multi-span beams. The experimental specimen examined is a twelve-span beam resting on simple supports, and disorder is achieved by altering the spacing between these supports in a random fashion. The beam is excited at one end by a sinusoidal moment and the steady state deflection is measured at several points along the beam. The spatial amplitude decay due to span length disorder is then calculated and compared to the theoretical predictions.

The paper is organized as follows. In Section 2 the theoretical model and the experimental specimen are described. The design requirements for the experiment, the experimental apparatus, and the measurement procedure are discussed in detail. In order to validate the experimental design the dynamics of three-span beams with equal and unequal support spacing are investigated experimentally in Section **3.** Since the self-averaging effect of span length disorder on the amplitude decay rate is not significant over three spans, the dynamics of ordered and disordered twelve-span beams are examined in Section **4.** Response shapes at resonance and non-resonance frequencies are measured and vibration localization is evidenced. In Section 5, the results of a wave propagation experiment conducted for the twelve-span beam. An incident wave packet is shown to be prevented from being transmitted along the disordered beam. In Section **6,** the spatial decay rate is estimated experimentally and compared to the theoretical localization factor derived for infinite multi-span beams. Section **7** concludes the paper.

2. Experimental Apparatus and Procedure

In this experiment we initially aimed to verify the occurrence of localization in a multi-span beam with weak interspan coupling. The motivation was that the degree of localization is known to increase as the coupling between spans is reduced [5]. **A** classical means of controlling interspan coupling is via rotational springs at the beam supports. However, although there are various experimental ways to achieve a restoring moment at a support, it proved virtually impossible to build the necessary number of such supports (equal to the number of spans plus one) with ***identical*** torsional rigidities —a critical design requirement. Therefore, we elected to perform our experiments on a beam resting on simple supports with zero nominal torsional rigidity. Although the localization phenomenon is less spectacular for this case of strong interspan coupling, the resulting experiment is actually conservative in the sense that if localization is shown to occur in the strong case then surely it will be stronger for weak interspan coupling.

2.1. The Experimental Setup

The experiment was performed on slender beams resting on simple supports whose spacing determined the span lengths. For the nominally ordered beam all span lengths were as equal as possible, while for the corresponding disordered beam the span lengths constituted a random sample from a uniform distribution of standard deviation, σ. The cross section, mass density, and bending stiffness were nominally uniform throughout the beam.

Designing and building a beam resting on "simple" supports is not a trivial process, because its dynamics are highly sensitive to the characteristics of the supports. Consequently, much care was given to the following requirements:

(a) Each simple support had to allow two degrees of freedom for the beam motion, namely rotation and longitudinal translation. Moreover, any torsional stiffness that might have arisen from the beam-support assembly had to be negligible compared to the beam stiffness, in order to satisfy the condition of no restoring moment.

(b) All supports had to be identical so that they would not create another uncontrollable source of disorder in the multi-span beam. Nonidentical support characteristics could cause localization in the ordered beam as well as in the beam with random span lengths.

(c) The beam had to be constrained at the support location in the transverse and lateral directions and the dynamics of the beam had to be insensitive to the the support fixtures. Moreover, in its static equilibrium state, the beam could not be subject to any residual tension or compression. This was avoided by eliminating any curvature other than that due to static defection. The latter was calculated and found to be negligible.

The experimental apparatus is presented schematically in Fig. 1 and a corresponding photograph is shown in Fig. 2. The slender beam was made of cold rolled low carbon steel with Young modulus $E = 30\,10^6\ lbf/in^2$ and density $\rho = 0.28\ lb/in^3$. Its width was $0.5\ in$ and its thickness $0.125\ in$. Note that the cold rolling process had the advantage of producing good quality finished surfaces. Moreover, the uniformity of the properties was excellent throughout the beam. The beam dimensions were chosen as a compromise between a flexible beam, which is very susceptible to mode localization but has the inconvenience of being too sensitive to initial stresses at the supports, and a stiff beam which is less sensitive to those stresses but is unlikely to exhibit significant vibration-localization in the frequency range of interest.

Several tests were performed on a three-span beam in order to reach a good design of the supports. A support was manufactured as a thick U-shape that could be fastened to a heavy base at its bottom surface. A thin pin of $\frac{1}{16}\ in$ diameter, made of steel with high rigidity, was allowed to ***go*** through the support and the beam simultaneously (see the photograph in Fig. 2). The beam's hole diameter was very slightly larger than the pin's diameter in order to allow the rotation of the beam around the pins while constraining the beam's vertical movement. The pins were lubricated in order to decrease friction. All supports were precisely positioned and fastened on the heavy base, which was designed as to allow moving the supports in order to adjust the span lengths. Note that because the beam deflection was very small, its longitudinal motion was negligible, and thus the beam-support assembly simulated simple supports effectively. Moreover, we avoided undesirable effects by first assembling the supports and the beam, and then fastening the supports to the base in such a way that they were all closely aligned, while checking that the beam rotates freely around the thin pins.

A preliminary experiment was performed on the three-

span beam prototype. Natural frequencies and modes shapes were obtained by modal analysis and compared to the theoretical ones (see Appendix A). The excellent agreement reached suggests that the design of the beam supports is satisfactory. The modal damping factors were also estimated and are given in Appendix A. In addition, the logarithmic decrement of the free response of the beam to an impulse force was determined. The damping coefficient extracted from these measurements averaged to $\xi = 0.5\%$. Thus the corresponding equivalent structural damping coefficient (loss factor) was $\eta = 2\xi = 1.0\%$, which is consistent with the average value of the three modal damping factors given in **A p** pendix **A.**

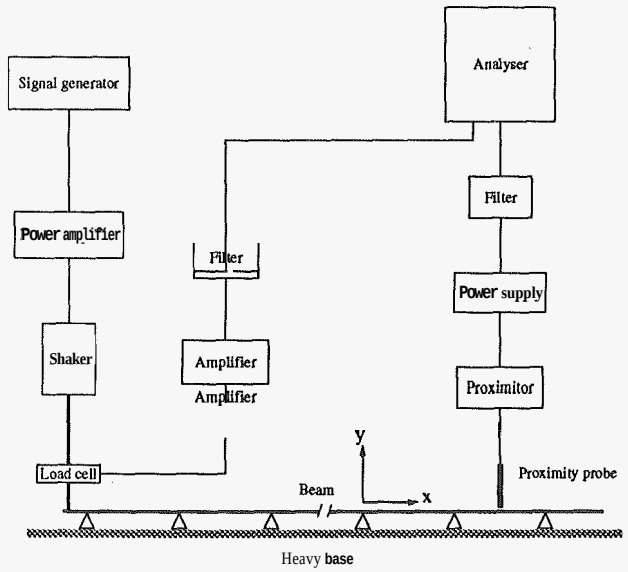

Figure 1, Experimental setup for forced vibration tests of the multi-span beam.

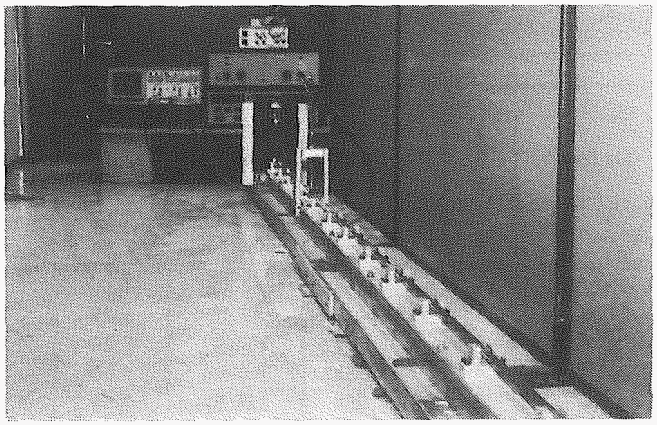

Figure 2. Photograph of the experimental bench. The twelve-span beam, proximity probe, shaker, and electronic equipment are shown.

2.2. The **Experimental Procedure**

Typically the dynamics of a structure are studied experimentally **by** identifying its natural modes of free vibration. These modes are obtained using modal analysis packages that process the measured acceleration, velocity or displacement of some points of the structure. This approach was found inadequate for the twelve-span beam, because of the high modal density which made the identification of the various modes difficult. (Note that this limitation of experimental modal analysis applies to all large periodic structures, or all structures with high modal densities). Therefore, we chose to examine the forced response of the beam to a harmonic excitation by measuring. its deflection at various locations and then plotting the amplitude and phase of the deflection versus the position along the beam. Since at a prescribed frequency, the steady state forced response dominates the beam vibration, the effect of the close natural frequencies is a lesser problem.

The beam was excited mechanically at one end by a B&K 4809 shaker and the excitation force was measured by a load cell mounted between the beam and the shaker. The excitation signal was generated by a vibration controller B&K 1050 and amplified by a B&K **2712** amplifier. Deflection of the steel beam was measured by a non-contacting proximity probe (8 mm Bently-Nevada), which could be positioned at several locations along the beam using a sliding device. The force and deflection signals could be viewed on an oscilloscope and recorded by a Computer-Aided Test System 2515 (GenRad).

The deflection-to-force frequency response function (FRF) of the system was measured directly by performing an incremental sine sweep. In such a sweep, an excitation signal is imposed at a driving frequency, and the excitation force and displacement response at that frequency are measured after a settling period during which the transient is allowed to decay. In our experiments it was necessary that the dynamic displacements remain small in order not to exceed the $\pm 1\,mm$ linear range of the probe. Therefore, the excitation force was fedback to the vibration controller (operating in closed loop), such that the deflection was kept within the desired range. Moreover, the sweeps covered the first and second frequency passbands separately in order to achieve a better resolution.

The resonance frequencies at which the frequency response function reaches a peak were precisely located. These are very close to the damped natural frequencies **of** the beam. The beam was then excited at each of these resonance frequencies and the maximum deflection amplitude as well as the phase at several points on the beam were recorded. The excitation of the experimental beam and the measurements were performed as follows:

1. **Moment *of excitation*:** The beam was excited by a sinusoidal force applied at the tip of a one-inch overhanging portion of the beam (see Fig. 1**).** This produced a moment applied to the left end support, $M(t) = M_o \sin(\omega t)$, where *w* is the frequency of excitation.

2. Deflection measuring device: The beam deflection was measured at several locations by a non-contacting proximity probe placed above the beam. Three points in each span were sufficient to capture the overall deflection shape at frequen-

cies in the first and second passbands. Since the supports were rigidly fastened to a heavy base, the beam deflection at the support locations was measured to be less than **1%** of the maximum amplitude of the beam. This was within the level of noise and the supports were therefore considered fixed with zero transverse displacement.

3. Deflection amplitude: Since the beam was slightly damped and the deflection amplitude small, steady state vibration was reached in less then one minute (during which no measurement was taken). The measured gap between the probe and the beam was divided by a dimensional calibration factor equal to **144** Volt/in. At a given position x, the time trace of the gap was recorded and the maximum deflection amplitude was calculated **as:**

$$Y(x) = \text{maximum deflection amplitude}$$

$$= \frac{1}{2}(\text{Gap}_{maxi} - \text{Gap}_{mini})$$

4. Deflection phase : The excitation force was measured by a load cell and recorded simultaneously with the deflection amplitude. At a given position x, the time delay $\tau(x)$ between the deflection and the force was measured and the corresponding phase was calculated as:

$$\Phi(x) = \text{deflection phase} = \tau(x) \times \omega$$

The deflection phase **was** rearranged to be in the interval $[-\pi, +\pi]$. In addition, the filter altered the phase by a frequency-dependent angle. The induced error in the phase was corrected by referring to the filter's characteristic chart.

3. Three-span Beam Results

The tests described above were first performed on a laboratory three-span beam. Even though strong localization was not exhibited by this short system, it allowed the verification of the validity and robustness of the experimental design and procedure, and particularly of the simple support design.

The ordered three-span beam was of a steel bar resting on four identical, equally spaced supports, with span length $l = 12\,in$. For the disordered three-span beam the supports were moved, the span lengths were $12\frac{1}{4}\,in$, $10\frac{15}{16}\,in$, $13\frac{5}{8}\,in$, corresponding to a disorder standard deviation $\sigma = 10.2\%$.

3.1. Resonance Frequencies

Experimental and theoretical frequency responses are displayed in Fig. **3** for the ordered beam. The frequency range comprises the first passband, that is, the lower three natural frequencies. The frequency response was recorded several times at various locations on the structure and good repeatability of the test was observed. Note that the experimental frequency response compares very well with the theoretical result calculated using the averaged experimental damping factor $\eta = 1\%$. The frequency responses were also compared for the disordered beam, and, similar to the ordered case, the theoretical calculation predicted the experimental measurements very well.

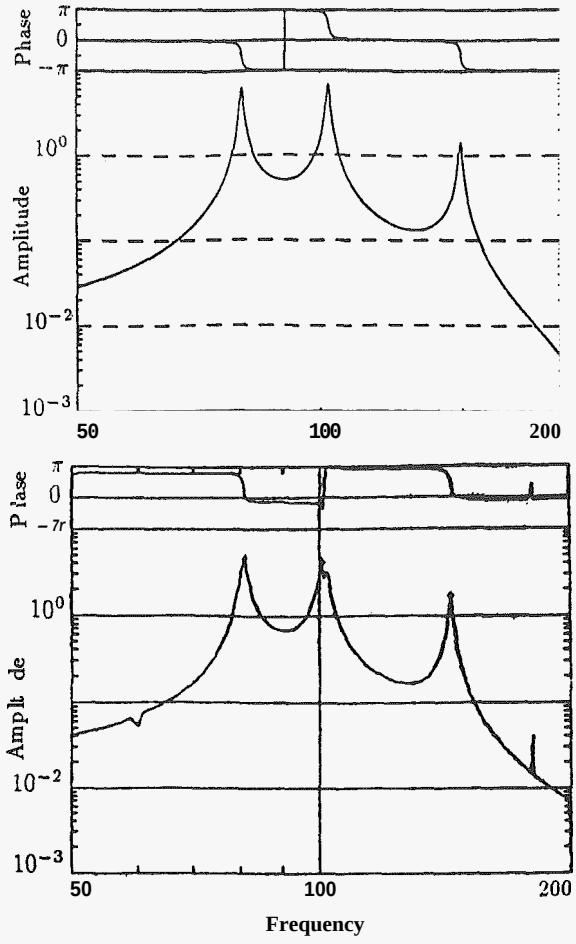

Figure 3. Frequency response (amplitude and phase) **for** an ordered three-span beam, measured at $4.5\,in$ from the left end of the 3rd span. Theoretical results for $\eta = 1\%$ (top) and experimental ones (bottom) are shown.

	No.	f_{theo} (Hz)	f_{exp} (Hz)	error %
Ordered	1	80.905	79.68	1.51
	2	103.681	99.80	3.74
	3	151.396	143.12	5.47
	4	323.621	305.00	5.75
	5	368.817	341.50	7.41
	6	452.481	417.20	7.80
Disordered	1	73.109	72.25	1.17
	2	93.659	92.43	1.31
	3	162.084	153.40	5.36
	4	282.522	268.60	4.93
	5	342.660	341.00	0.48
	6	487.929	460.60	5.60

Table 1. Theoretical and experimental resonance frequencies of an ordered and a disordered three-span beam with $\sigma = 10.2\%$ $(\eta = 1\%)$.

The lower six theoretical and measured resonance frequencies are given in Table **1.** They are predicted with a maximum error of **7.8%** for the ordered beam and 5.6% for the

disordered beam. We notice that the resonance frequencies of the disordered beam have shifted from the ordered beam frequencies by approximately 10%, that is, by about the disorder level —a known result [11]. For this particular realization of disorder, the first and second resonance frequencies are lower than for the ordered beam, while the third is higher. This is not general since another realization of disorder would give a different frequency change.

3.2. Forced Response Shapes

The response shapes at the resonance frequencies are plotted in Fig. **4.** Since there is a slight difference between measured and calculated resonance frequencies, the experimental and the theoretical deflection shapes correspond to the measurement and calculated frequencies, respectively. Moreover, the experimental deflection measurements are normalized such that they can be compared to the theoretical values. Very good agreement is shown for all the responses in the first two passbands. In some regions of the beam, a small discrepancy is noticeable between the measured and the calculated vibration pattern. This is attributed mainly to errors in measurement and to the small initial curvature of the beam in the direction normal to the motion.

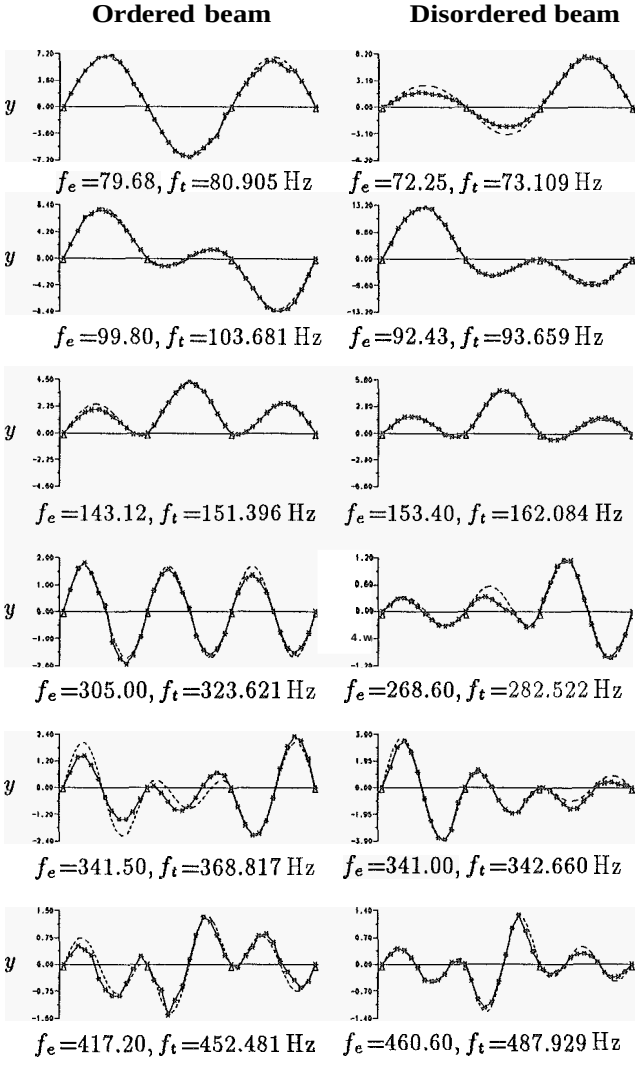

Figure 4. Forced response amplitude at the lower six resonance frequencies of ordered and disordered three-span beams. Theoretical results with $\eta = 1\%$ (- - -) and experimental ones (–*–) are shown. The disorder standard deviation is $\sigma = 10.2\%$.

By comparing the responses of the disordered and ordered beams in Fig. **4,** we notice in the disordered case the occurrence of localization and the confinement of vibrational energy to mostly one of the spans for each resonance frequency. Moreover, it is interesting to note that at the 1st and 4th resonance frequencies it is the longest (right-end) span that experiences the largest amplitude, while at the 2nd and 5th resonance frequencies it is the second longest (left-end) span, and at the 3rd and 6th resonance frequencies it is the shortest (middle) span. This can be explained by invoking that the longest span has the lowest individual fundamental natural frequency, and thus attracts most of the vibrational energy of the first mode. Similarly the shortest span, having the highest individual fundamental natural frequency, attracts most of the vibrational energy of the third mode. The same reasoning holds for the higher mode groups.

The above results demonstrate that the experimental measurements are consistent with the theoretical calculations. It confirms that the theoretical model captures the dynamics of the specimen beam and that the experimental procedure is adequate. In particular, the interspan coupling for the experimental beam is as strong as taken in the theoretical model and the measured structural damping factor is realistic. This preliminary experiment also evidences the occurrence of mode localization (albeit not very strongly) for the three-span beam.

4. Twelve-§pan Beam Results

Although the results in Section **3** reveal the occurrence of localization effects, the three span beam has too few spans to allow an estimation of the average rate of amplitude decay, the localization factor. Next the number of spans is therefore increased to twelve.

The objective of the twelve-span beam experiment are twofold: First, to verify that strong localization occurs by comparing the forced response shapes of ordered and disordered beams and second, to measure the average rate. of spatial amplitude decay and compare it to the calculated localization factor for infinite multi-span beams [5].

4.1. The Ordered Beam

The ordered twelve-span beam rests on thirteen identical supports equally spaced by 10 *in*. All supports were positioned on to and attached to the heavy base by, making sure not to induce unwanted static stresses in the beam, which turned out to be a delicate matter. Steps such as tuning and then testing had to be repeated several times until satisfactory results were obtained. When a satisfactory tuning was obtained, however, the beam dynamics became insensitive to minor disturbances and the setup was robust. At this point we were confident that the twelve-span beam was "perfectly" ordered.

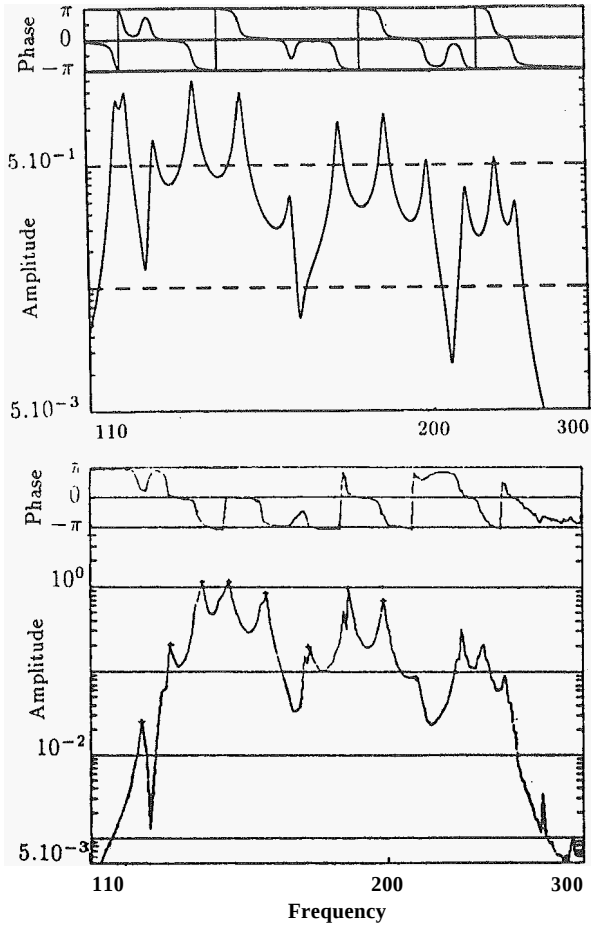

Figure 5. Frequency response (amplitude and phase) of an ordered twelve-span beam, measured at the middle of the 9th span. Theoretical results for $\eta = 1\%$ (top) and experimental ones (bottom) are shown.

1st Passband			
No.	f_{theo} (Hz)	f_{exp} (Hz)	error %
1	116.491	116.50	0.01
2	118.500	118.71	0.18
3	125.399	128.88	2.70
4	135.674	135.46	-0.16
5	149.022	147.95	-0.72
6	164.315	163.12	-0.73
7	181.739	177.80	-2.22
8	199.654	192.85	-3.53
9	217.498	210.50	-3.32
10	234.947	227.86	-3.11
11	249.478	240.50	-3.73
12	259.555	251.15	-3.35
2nd Passband			
No.	f_{theo} (Hz)	f_{exp} (Hz)	error %
13	465.251	455.31	-2.18
14	470.245	458.65	-2.53
15	484.198	469.74	-3.08
16	504.896	482.13	-4.72
17	530.226	502.26	-5.57
18	558.603	526.39	-6.12
19	588.833	549.46	-7.17
20	619.859	574.48	-7.90
21	650.506	600.80	-8.27
22	679.198	619.91	-9.56
23	703.631	640.76	-9.81
24	720.624	654.11	-10.17

Table 2. Theoretical and experimental resonance frequencies of an ordered twelve-span beam $(\eta = 1\%)$.

Similarly to the three-span beam, the resonance frequencies of the twelve-span beam are obtained by precisely locating the peaks of the frequency response function in Fig. 5. These values are compared to the theoretical ones in Table 2. Note that the error is less than 3.4% for the 12 modes in the first passband and less than 10.2% for those in the second passband. If a 10.2% error in the resonance frequencies seems large, one must bear in mind that in the second band some of the frequencies are closely spaced. In the first band the first three theoretical values are lower than the experimental ones and the other nine are higher. In the second band the experimental values are always lower than the theoretical ones. This may be due to the fact that at higher frequencies the pins which make up the supports become more flexible, thereby softening the multi-span beam. softer relative to the beam.

Next, the ordered beam is excited near its first support by a sinusoidal moment of amplitude chosen such that the beam deflection remains in the linear range. The frequency of excitation is either in stopbands or in passbands. In a passband, the frequency can be either a **resonance** or a **non-resonance** frequency. Thus the following three cases are distinguished:

Case 1: The excitation frequency belongs to a stopband. Recalling that the first natural frequency of each mode group constitutes the lower passband edge and that the 12th (and last) natural frequency in the group is smaller than the upper passband edge [5], we can use Table 2 to define the frequency stopbands approximately. For the first stopband, $0 < f_{exp} < 116$ Hz, and for the second stopband, 265 Hz $< f_{exp} <$ 450 Hz (accounting for experimental errors). Figure 6 depicts typical theoretical and experimental response shapes at selected stopband frequencies near the passband edges. For all frequencies a strong spatial decay is observed. Indeed, the measured deflection amplitude in the last four spans is of the order of the equipment noise. Note that the decay is mainly due to the off resonance condition which characterizes the stopbands, while damping has only a small contribution to this amplitude attenuation [4,5].

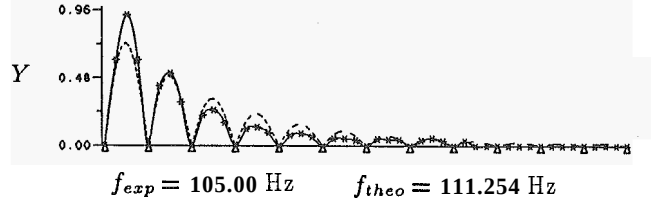

$f_{exp} = 105.00$ Hz $\quad f_{theo} = 111.254$ Hz

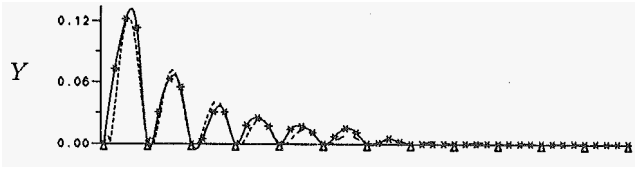

$f_{exp} = 283.42$ Hz $\quad f_{theo} = 283.421$ Hz

Figure 6. Forced response maximum amplitude at frequencies in the stopbands of a damped ordered twelve-span beam. Theoretical results with $\eta = 1\%$ (- - -) and experimental ones (−∗−) are shown.

Case 2: The excitation frequency is a resonance frequency of the twelve-span beam (see Table **2).** Figure 7-a compares the theoretical and experimental deflection amplitude and phase at selected resonance frequencies in the first passband. The experimental deflections were recorded at three points on each span. Theoretical values were calculated using the estimated damping factor $\eta = 1\%$. Note that at the first fundamental natural frequency the spatial decay due to damping is most significant. This is because the effect of damping is strongest near the edges of the passband and the left passband edge coincides with the first resonance frequency [5]. However, the amplitude decay is much stronger in the experimental case. Our explanation **for** this behavior is that near the passband edges, the rate of decay due to damping is very sensitive to the frequency position in the passband. In our experiment it is possible that small errors ***or*** very small defects placed the first resonance frequency very slightly inside the stopband, which would explain the strong spatial decay [4]. At all other resonance frequencies the spatial decay is barely noticeable in the response shape, which means that damping has little effect on the spatial attenuation of the response. Note the general very good agreement between experimental and theoretical deflection amplitudes **as** well as phases. Figure **7-b** depicts the theoretical and experimental deflection amplitudes at **four** resonance frequencies in the second passband. Experimentally we observed considerable interactions between the close neighboring modes and the individual mode resonant responses could not be identified accurately.

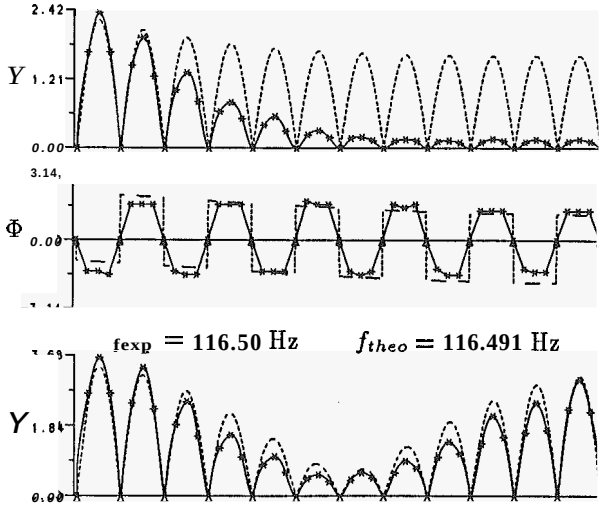

$f_{exp} = 116.50$ Hz $\quad f_{theo} = 116.491$ Hz

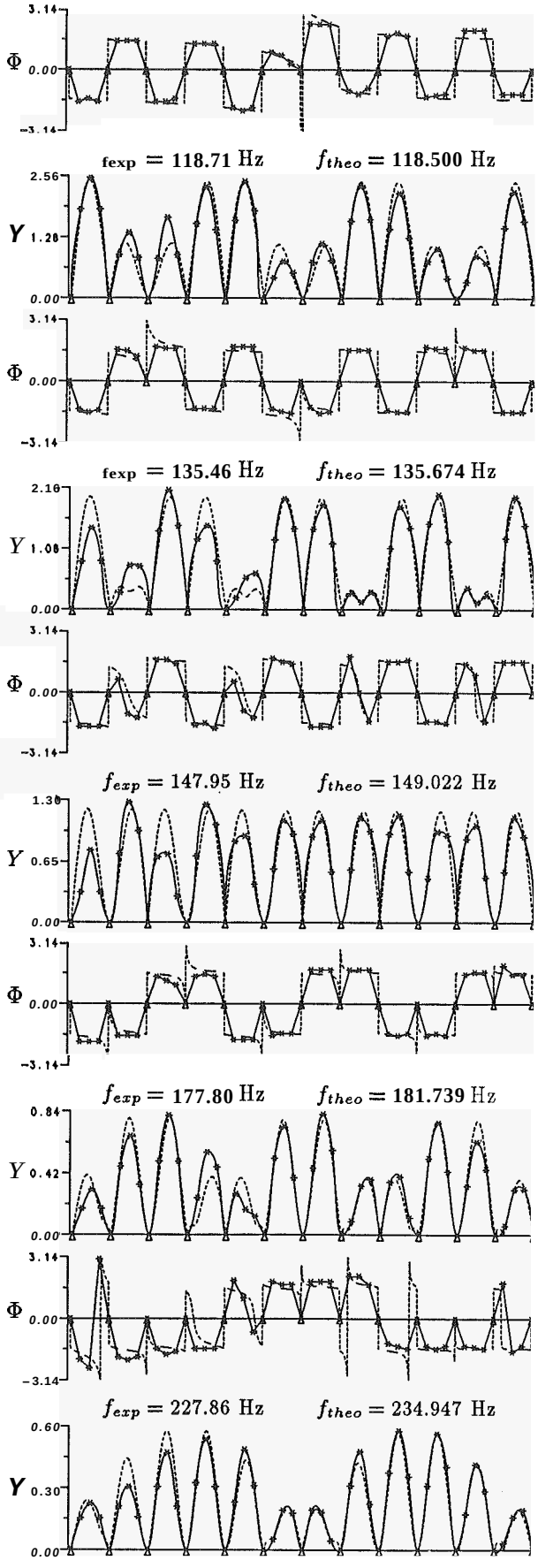

$f_{exp} = 118.71$ Hz $\quad f_{theo} = 118.500$ Hz

$f_{exp} = 135.46$ Hz $\quad f_{theo} = 135.674$ Hz

$f_{exp} = 147.95$ Hz $\quad f_{theo} = 149.022$ Hz

$f_{exp} = 177.80$ Hz $\quad f_{theo} = 181.739$ Hz

$f_{exp} = 227.86$ Hz $\quad f_{theo} = 234.947$ Hz

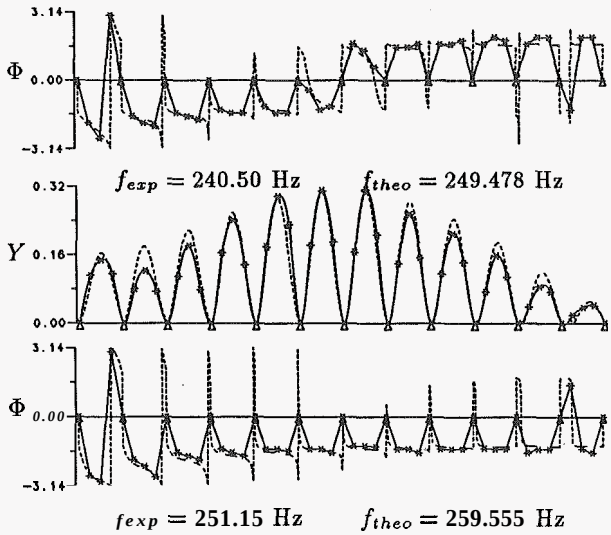

Figure 7-a. Maximum forced response amplitude and phase at selected resonance frequencies in the first passband of a damped, ordered, twelve-span beam. The theoretical results with $\eta = 1\%$(- - -) and experimental ones (–*–) are shown.

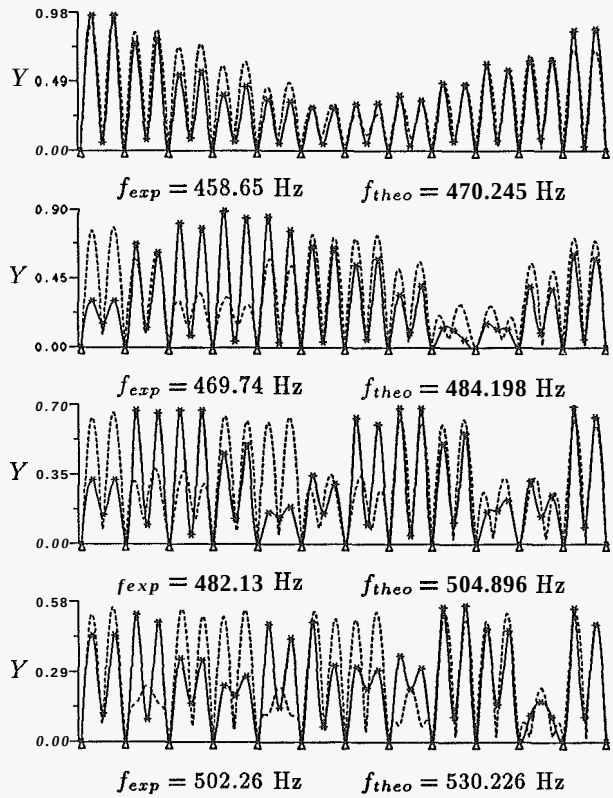

Figure 7-b. Maximum forced response amplitude at selected resonance frequencies in the second passband **of** a damped, ordered, twelve-span beam. Theoretical results with $\eta = 1\%$(- - -) and experimental ones (–*--) are shown.

Case 3: The *excitation frequency lies* in a passband, between *two* resonance frequencies. This allows **us** to examine the response when more than one natural mode is excited. Recall that the experimental and theoretical excitation frequencies need not be equal, but rather account for the discrepancies listed in Table **2.** For a selected theoretical frequency, this was achieved by using linear interpolation to determine the corresponding experimental excitation frequency. Figure **8** displays the theoretical and experimental deflection amplitudes at two selected frequencies. Even though the frequency of excitation is away from a resonance frequency, the influence of the closer natural modes **is** exhibited by the overall response shape.

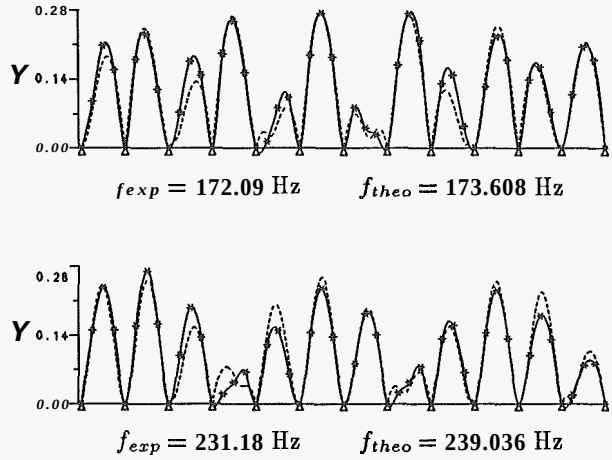

Figure 8. Forced response maximum amplitude at nonresonance frequencies in the first passband of a damped, ordered, twelve-span beam. Theoretical results with $\eta = 1\%$ (- - -) and experimental (–*–) ones are shown.

For the three above cases, a very good agreement was obtained between the theoretical and experimental deflection amplitudes. The agreement for the phases was considered satisfactory since only three experimental data points per span were used, which was not sufficient to capture accurately the rapid variation of the phase along the spans. We also noticed that the experimental amplitudes are consistently lower than the theoretical ones for the three spans closest to the excitation source. This is due to the excitation device attached near the beam's end, which increases the stiffness of the first few spans and therefore reduces their deflection amplitude. Another source of discrepancy between theoretical and experimental results may be the light frictional damping at the supports.

4.2. The Disordered Beam

The beam was disordered by moving the inner supports in a random fashion and keeping the total length constant. This necessitated drilling small holes at the new support locations in order to obtain precisely the span lengths desired. The set of random span lengths is given in Table **3.** The new supports were carefully fastened and aligned, as for the ordered beam.

Span No.	Length (*in*)
1	9.8
2	9.35
3	11.3
4	10.0
5	10.9
6	9.05
7	10.3
8	8.7
9	9.7
10	11.1
11	10.5
12	9.3

Table 3. Set of random span lengths with a mean $\bar{l} = 10.0\,in$ and $\alpha = 8.36\%$.

No.	f_{theo} (Hz)	f_{esp} (Hz)	error %
1	110.782	116.16	4.85
2	112.811	117.38	4.05
3	128.027	131.70	2.87
4	141.079	143.90	2.00
5	148.131	147.48	-0.44
6	156.880	156.77	-0.07
7	188.218	186.00	-1.18
8	203.020	197.97	-2.49
9	217.934	212.25	-2.61
10	238.331	225.80	-5.26
11	250.551	244.35	-2.48
12	285.167	274.26	-3.82
13	429.568	411.70	-4.16
14	435.969	430.70	-1.21
15	475.338	464.40	-2.30
16	519.792	503.10	-3.21
17	529.398	517.40	-2.27
18	538.980	575.30	6.74
19	613.463	581.80	-5.16
20	623.215	615.90	-1.17
21	655.637	705.50	7.61
22	704.169	711.50	1.04
23	734.460	769.80	4.81
24	814.008	888.10	9.10

Table 4. Theoretical and experimental resonance frequencies of a disordered twelve-span beam with $\alpha = 8.36\%$ and $\eta = 1\%$.

The disordered beam was driven at the same location as the ordered beam by the exciter and the resonance frequencies were again obtained from the frequency response function. However, in this disordered case it was difficult to locate all twelve peaks from a single measurement location, because the measuring device located in the 9th span was not able to detect the very small deflection amplitudes of that span at some resonance frequencies. Therefore, several frequency response functions recorded at various locations were used to determine all resonance frequencies in the first two mode groups. These frequencies are compared to the theoretical results in Table 4. Note that the discrepancy between theoretical and experimental results is less than 5.3% for the first group and 9.1% for the second group.

Similarly to the ordered case, the maximum amplitude and the phase of the forced response were measured and plotted. They are compared to the theoretical results for selected resonance frequencies in the first passband in Fig. 9-a. First, it is worth observing the very good general agreement between measurement and theory. The agreement is good even for the phases, bearing in mind that the deflection **was** recorded at only three points on each span and that point interpolation is not as accurate for the phase as for the amplitude. The maximum amplitude of the response at four resonance frequencies from the second mode group are displayed in Fig. 9-b. Figure 10 shows the response shapes at some selected non-resonance frequencies.

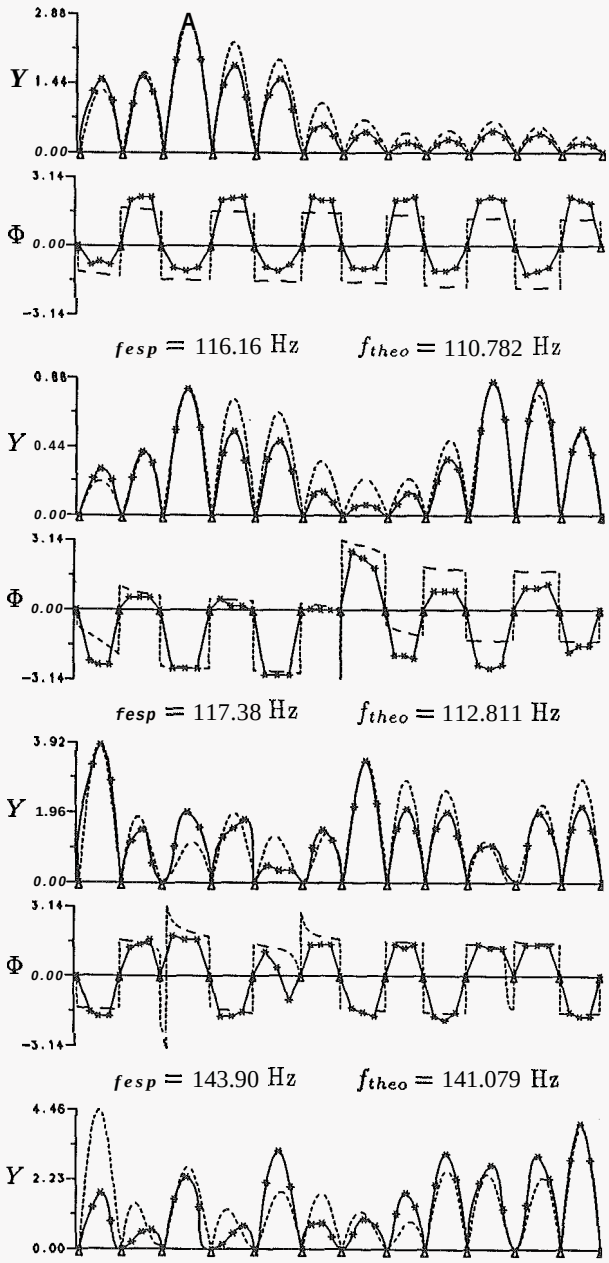

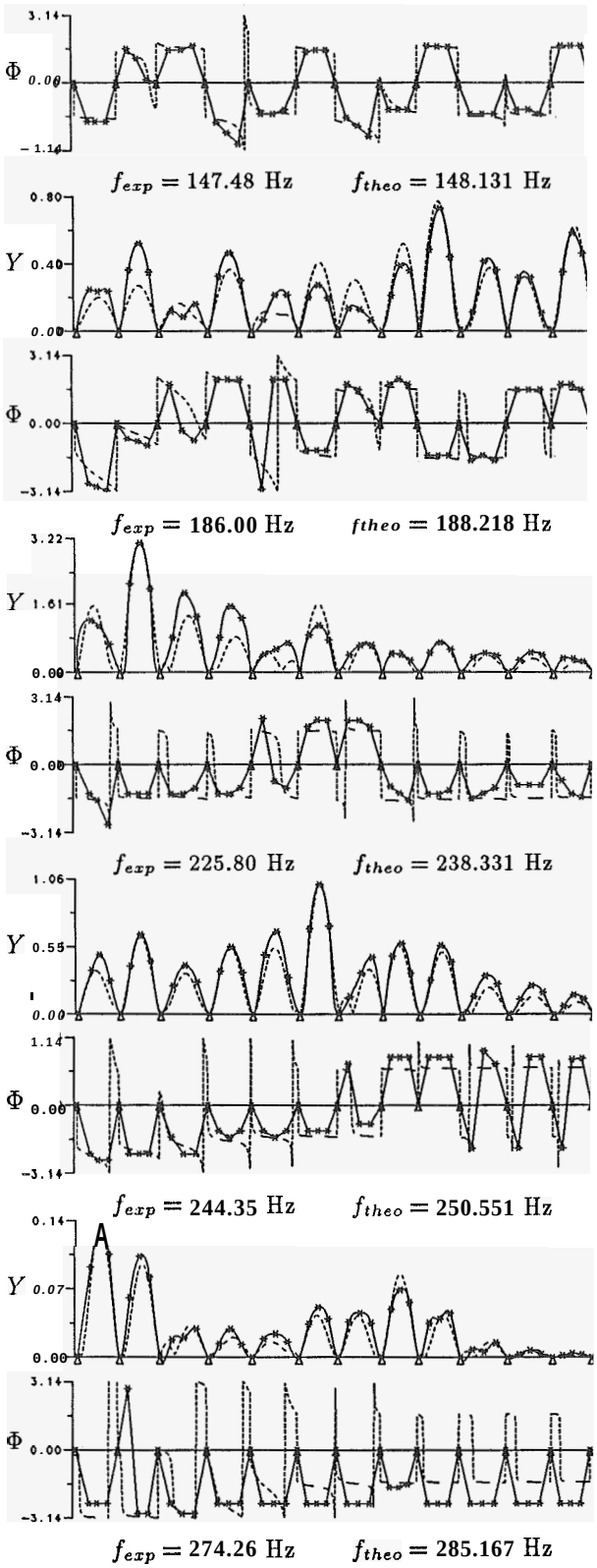

Figure 9-a. Maximum forced response amplitude and phase at selected resonance frequencies in the first passband of a damped, disordered twelve-span beam. Theoretical results with $\eta = 1\%$(- - -) and experimental ones (−∗−) are shown. The disorder standard deviation is $\sigma = 8.36\%$.

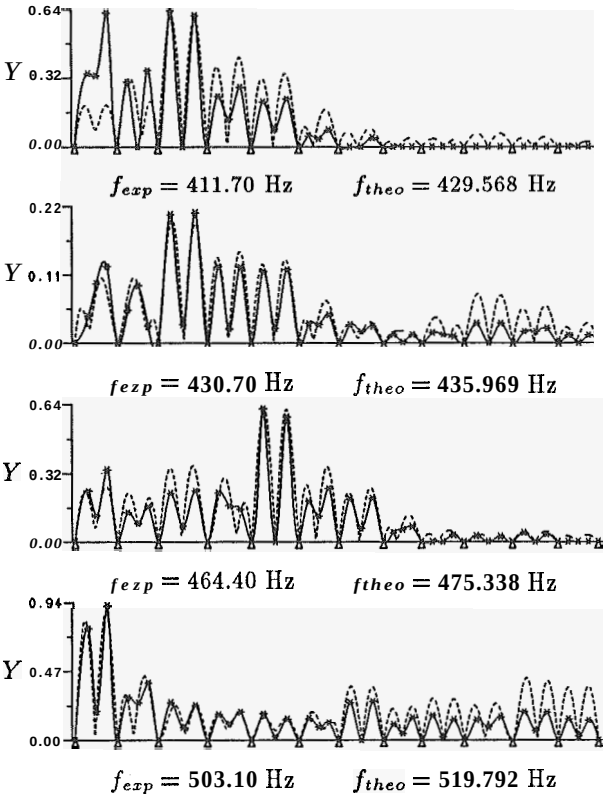

Figure 9-b. Maximum forced response amplitude at the resonance frequencies in the second passband of a damped, disordered twelve-span beam. Theoretical results with $\eta = 1\%$ (- - -) and experimental ones (−∗−) are shown. The disorder standard deviation is $\sigma = 8.36\%$.

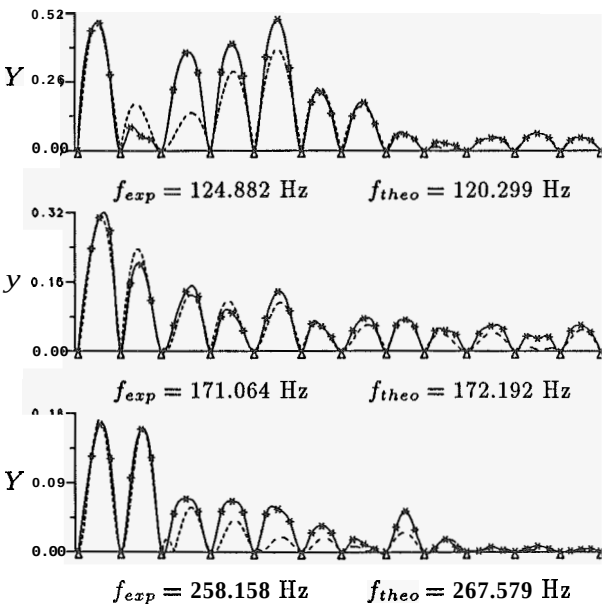

Figure 10. Forced response maximum amplitude at selected non-resonance frequencies in the first passband of a damped disordered twelve-span beam. Theoretical results with $\eta = 1\%$ (- - -) and experimental ones (−∗−) are shown. The disorder standard deviation is $\sigma = 8.36\%$.

In order to depict the disordered twelve-span beam motion, Figure 11 shows the theoretical and experimental response shapes, for selected resonance frequencies, at an instant of time, chosen as to coincide nearly with the maximum deflection envelope. Note that for this lightly damped beam, the forced response shapes in Fig. 11 are very similar to the corresponding mode shapes. Hence they are close to the localized modes of the disordered twelve-span beam.

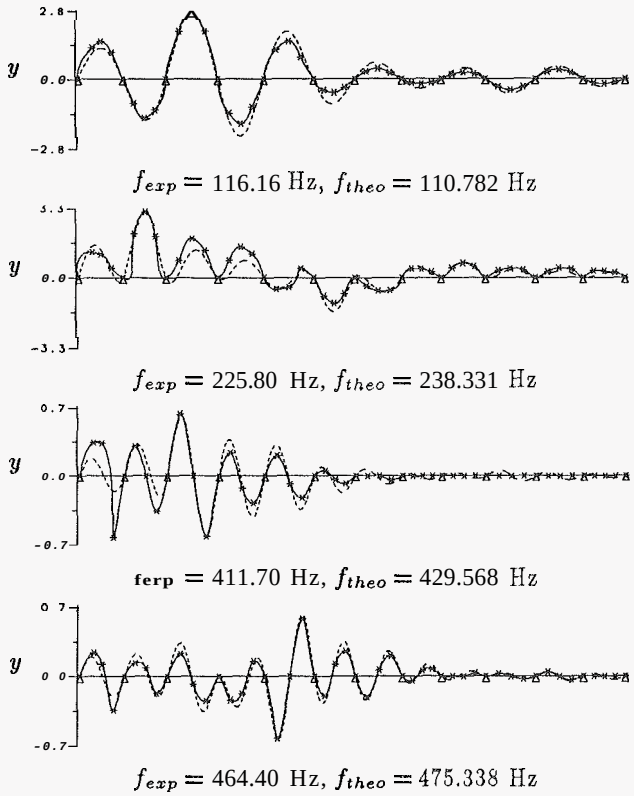

Figure 11. Localized forced responses at selected resonance frequencies for a damped, disordered twelve-span beam. Theoretical results with $\eta = 1\%$(- - -) and experimental ones (−∗−) are shown. The disorder standard deviation is $\sigma = 8.36\%$.

4.3. Discussion of Experimental Results

The difference between the responses in Fig. 7 for the ordered beam, which agree very well with periodic structure theory, and those in Fig. 9 for the disordered beam, where vibrations are localized, is striking. Our experiment demonstrates clearly that when the disordered beam is excited at one end by a harmonic moment, localization may manifests itself by greatly reducing the energy transmitted along the beam to the other end. However, notice that the forced response is localized at some frequencies while it remains extended at others. For example, the forced response shapes at resonance frequencies 1, 10, and 12 reveal very clear localization, producing a greatly reduced vibration amplitude in the last few spans. Furthermore, responses at most resonance frequencies in the second group are more strongly localized than in the first group. For example, at frequencies 13 and 15 almost no vibration energy is transmitted to the last span. Also note that, the responses of the disordered beam, at those resonance frequencies which have moved inside the stopbands of the associated ordered beam (*e.g.*, 1st and 13th frequencies) are more strongly localized.

The amplitude of the force of excitation was kept the same for both ordered and disordered beams and for all frequencies within each passband. In the second passband, the force amplitude was a little higher in order to obtain a large enough beam deflection that could be measured accurately. The results of Figs. 7 and 9 show that when localization occurs, the amplitude may be greatly reduced in some spans but increased in others. For example, at the tenth resonance frequency Fig. 7-a shows that the maximum amplitude for the ordered beam is approximately 0.8 (in displacement units), while in Fig. 9-a the amplitude in the second span of the disordered beam is as high as 3.2 —a four-fold increase. On the other hand, consider the responses at the 14th resonance frequency in Figs. 7-b and 9-b. The maximum amplitude for the ordered beam is 0.94 while it is approximately 0.22 in the third span: hence the vibration amplitude has been reduced by a factor of 4. Moreover, almost no vibration has been transmitted to the second half of the beam.

We also note in Figs. 7-a and 9-a the phase is practically the same for both ordered and disordered beams; hence the phase is not as much affected by the disorder as the amplitude is.

5. Transient Response to a Wave Packet

Perfectly periodic structures have the property of allowing the propagation of harmonic waves in frequency passbands, while in disordered structures these waves are scattered and therefore spatially attenuated. Experimental tests were performed to verify this phenomenon for the twelve-span beam. The tests consisted of sending a harmonic wave packet from one end of the beam and measuring the waves transmitted to the other end before they reflect at the system boundary. The wave packet was generated by exciting the beam at its left end by a sinusoidal time-varying moment at some frequency, for a duration of approximately one-half of one second.

It is appropriate to mention here some experimental aspects of recording the wave signals for the twelve-span beam. In contrast to the vibration tests performed above, only a short duration of the time trace of the signal needed to be analyzed. The simple setup chosen to record this transient event consisted of an oscilloscope with a storage capability. The traces were stored on the phosphorus screen, from which a hard copy generated. This recording technique required an external triggering with a short delay.

The deflection amplitude was measured at the 11th span (near the right-end) and its time trace recorded on the oscilloscope simultaneously with the excitation signal, which was given by a force transducer mounted between the beam and the shaker. Illustrative force and deflection signals recorded on the oscilloscope are displayed in Fig. 12. In order to make a qualitative comparison, we should point out that the scale of the graphs (not shown) is the same for all force signals and, respectively, for all deflection signals. For the ordered beam, the plots reveal that no wave amplitude is transmitted to the 11th span when the excitation frequency lies in a stopband (f = 116 Hz and f = 280 Hz). However, for

frequencies in the passbands ($f = 172$ Hz and $f = 225$ Hz) the amplitude at the middle of the 11th span is large, which reveals that energy is nearly fully transmitted to the end of the beam.

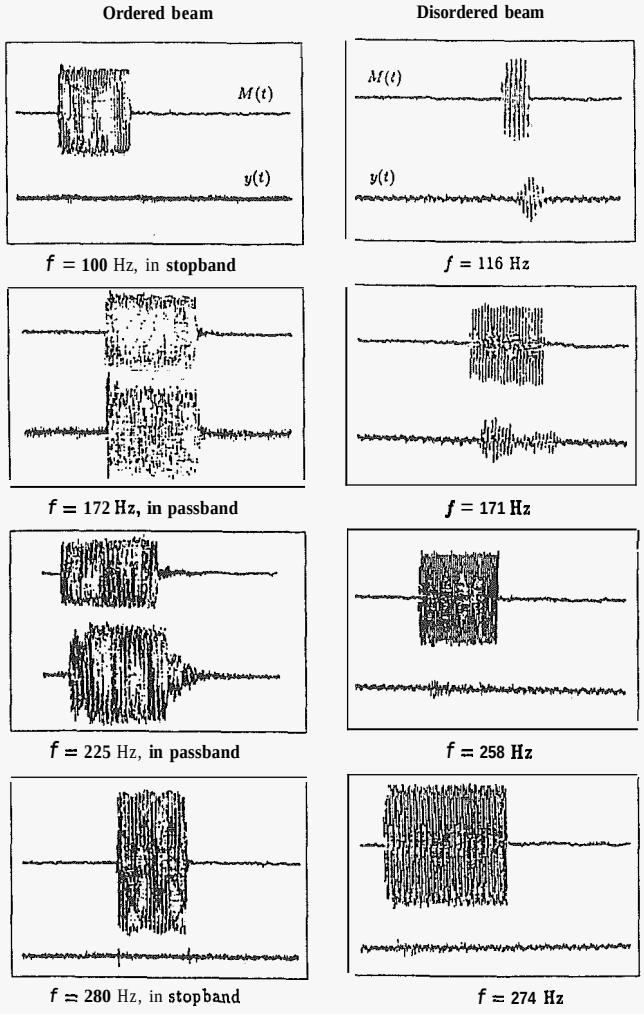

Figure 12. Transient response of the twelve-span beam to a sinusoidal wave packet. The excitation moment is applied at the left end and the deflection amplitude is measured at the 11th span. The ordered (left) and disordered (right) beam responses are shown.

These tests were repeated on the disordered beam for several excitation frequencies in the same range. Figure 12 shows that the amplitude of the 11th span is always very small or zero, that is, the vibration amplitude is not being transmitted along th beam but confined near the source of excitation. This is a demonstration of strong wave localization in the disordered beam. We should mention that if the disordered beam were excited at a frequency for which localization does not occur, the response would feature a significant amplitude at the 11th span.

6. Estimation of the Spatial Decay Rate

We are now ready to quantify the degree of localization in the experimental beam and compare the result to the theoretical prediction. This is made possible by the fact that the forced response of the multi-span beam is known to decay exponentially, in an average or asymptotic sense, away from the excited end (see [4,5] for details).

In order to estimate the spatial decay rate, γ_N, in a finite N-span beam, we attempt to fit, in a least square sense, an exponential envelope to the N values of the maximum deflection amplitudes within each span. If the vibration amplitude decays away from, say, span m, $1 \leq m \leq N$, we choose to fit the exponential envelope over the longest portion of the beam (the m-span or the $(N - m)$-span portion) where localization occurs. For example, for the m-span portion, the exponential envelope is given by $a(n) = Ae^{-\gamma_N(n-m)}$, where $a(n)$ is the maximum deflection amplitude in span n.

Mode No.	γ_{12}	γ	% error
1	0.35	0.298	14.86
$f^* = 124.88$ Hz	0.45	0.173	61.56
3	0.39	0.129	66.92
6	0.21	0.071	66.19
$f^* = 171.06$ Hz	0.17	0.066	61.18
10	0.22	0.141	35.91
11	0.27	0.177	34.44
$f^* = 258.16$ Hz	0.33	0.257	22.12
13	0.58	0.392	32.41
14	0.40	0.361	9.75
15	0.52	0.265	49.04
16	0.30	0.209	30.33

Table 5. Spatial decay rate, γ_{12}, estimated from selected experimental response shapes that feature localization. The localization factor γ is obtained from Monte Carlo simulation by averaging over 1000 realizations of randomly disordered 100-span beams (for $\eta = 1\%$ and $\sigma = 8.36\%$). The $*$ denotes a non-resonance frequency.

Table 5 gives the experimental decay rate, γ_{12}, estimated from the response shape of the disordered twelve-span beam excited at selected resonance frequencies. The results are compared to the localization factor which is defined as an asymptotic, or an average rate of decay in an infinite disordered multi-span beam and which is obtained obtained by performing a numerical Monte Carlo simulation (see [4,5]). In this simulation the spatial decay rate is estimated by averaging over 1000 realizations of randomly disordered 100-span beams. Notice that the experimental decay rate is approximately of the order of the localization factor. The discrepancy is mainly due to the effect of the boundary conditions and to the fact that 12 spans is not a sufficient number of bays for the self-averaging of the decay to occur. This is confirmed by the better agreement between the estimated decay rate and the localization factor for frequencies at which the localization is stronger (see the response shapes in Figs. 7 and 9). Although the agreement between experimental and theoretical results is only qualitative here, it suggest that the average localization factor can provide rough but valuable information regarding the degree of localization in the finite disordered twelve-span beam.

7. Conclusion

In this paper we have evidenced experimentally the occurrence of vibration localization in disordered multi-span beams. Very good quantitative agreement was obtained between the experimental results and the theoretical findings presented in references [4,5]. The following conclusions are reached:

- The spatial localization of the steady-state harmonic response to an end excitation was observed in the disordered twelve-span beam. In some cases for the dis ordered beam, the deflection amplitude in one of the spans increased by a factor of four as compared to the ordered beam response, while only vibration amplitude of the level of noise was transmitted to the span farthest from the excitation.
- At most frequencies in the passbands, the spatial decay due to damping in the ordered beam was negligible compared to the spatial decay due to disorder in the disordered beam.
- Localization was stronger for frequencies which lie in the second passband than for those in the first passband. This agrees with the theoretical findings that predict an increase of the localization strength with the passband number.
- The spatial decay rate was estimated experimentally by fitting an exponential envelope to the localized response shapes. When the region of confinement of the response is small, fair agreement was observed between the experimental decay rate and the localization factor for an infinite disordered multi-span beam. This suggests that the localization factor calculated for an infinite structure provides a fair characterization of the degree of localization for typical realizations of finite multi-span beams.

References

1. Hodges, C. H., **1982,** "Confinement of Vibration by Structural Irregularity," **Journal of Sound and Vibration,** Vol. **82,** No. **3,** pp. **411-424.**

2. Bendiksen, O. O., **1987,** "Mode Localization Phenomena in Large Space Structures," **AIAA Journal,** Vol. **25,** No. **9,** pp. **1241-1248.**

3. Kissel, G. J., **1988,** "Localization in Disordered Periodic Structures,'' **Ph.D. Dissertation, Massachusetts Institute** of **Technology.**

4. Bouzit, D., and Pierre, C., **1993,** "Vibration Confinement Phenomena in Disordered, Multi-span Beams with Damping," **Proceedings** of **the** *14th* **Biennial** *ASME* **Conference on Mechanical Vibration and Noise,** Albuquerque, New Mexico.

5. Bouzit, D., and Pierre, C., **1992,** "Vibration Confinement Phenomena in Disordered, Mono-coupled, Multi-span Beams," *ASME* **Journal** of **Vibration and Acoustics,** Vol. **114,** No. **4** pp. **521-530.**

6. Hodges, C. H., and Woodhouse, J., **1983,** "Vibrations Isolation from Irregularity in a Nearly Periodic Structure: Theory and Measurements," **Journal of the Acoustical Society** of **America ,** Vol. **74,** No. **3,** pp. **894-905.**

7. Pierre, C., Tang, D. M., and Dowell, E. H., **1987,** "Localized Vibrations of Disordered Multi-Span Beams: Theory and Experiment," **AIAA Journal,** Vol. **25,** No. **9,** pp. **1249-1257.**

8. Roy **A. K.,** and Plunkett R., **1985,** "Dispersive Bending Waves in Uniform Bars," **Experimental Mechanics ,** Vol. **25,** No. **3,** pp. **308-311.**

9. Roy **A.** K., and Plunkett R., **1986,** "Wave Attenuation in Periodic Structures," **Journal of Sound and Vibration,** Vol. **104,** No. **3,** pp. **395-410.**

10. Levine-West M. B., and Salama M. **A., 1992,** "Mode Localization Experiments on a Ribbed Antenna,'' **Proceedings of the 33rd** *AIAA/ASME/ASCE/AHS/ASC* **Structures, Structural Dynamics, and Materials conference.** Dallas, TX, pp. 2038-2047.

11. Pierre, *C.,* and Dowell, E. H., **1987,** "Localization of Vibrations by Structural Irregularities," **Journal of Sound and Vibration,** Vol. **114,** No. **3,** pp. **549-564.**

APPENDIX A: Modal Analysis Results

Natural frequencies and modes shapes of an ordered three-span beam were obtained experimentally. The mode shapes were estimated using the Multi Degree Of Freedom method with circle fitting. The experimental results are consistent with the theoretical predictions, **as** shown in Table **A-1** and Fig. **A-1.** The modal damping factor was estimated for each mode shape.

Mode	f_{theo}	f_{exp}	error %	η%
1	**80.05**	**81.48**	**1.75**	**1.75**
2	**102.62**	**103.45**	**0.80**	**0.84**
3	**149.76**	**147.85**	**-1.29**	**0.44**

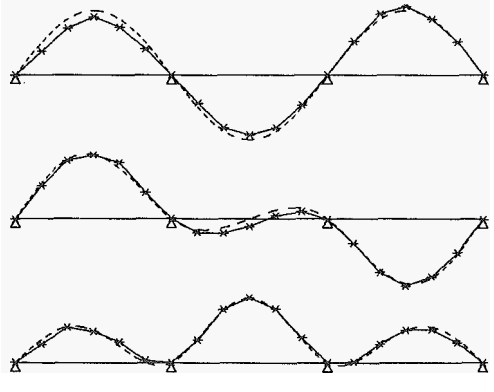

Figure A-1. First three mode shapes for an ordered three-span beam. Both theoretical (- - -) and experimental (–*–) modes are shown.